Si/TiO₂ Tandem-Junction Microwire Arrays for Unassisted Solar-Driven Water Splitting

Matthew R. Shaner,[a,b] **Matthew T. McDowell,**[a,b] **Alex Pien,**[b] **Harry A. Atwater,**[b,c,z]
and Nathan S. Lewis[a,b,*,z]

[a]*Division of Chemistry and Chemical Engineering, California Institute of Technology, Pasadena, California 91125, USA*
[b]*Joint Center for Artificial Photosynthesis, California Institute of Technology, Pasadena, California 91125, USA*
[c]*Thomas J. Watson, Sr. Laboratories of Applied Physics, California Institute of Technology, Pasadena, California 91125, USA*

Tandem-junction microwire array photoelectrodes have been fabricated by coating np$^+$-Si radial homojunction microwire arrays sequentially with fluorine-doped tin oxide (FTO) and titanium dioxide (TiO$_2$). These photoelectrodes effected unassisted water splitting under simulated 1 Sun conditions with an open-circuit potential (E_{oc}) of -1.5 V vs the formal potential for oxygen evolution, $E^{0\prime}$(OH$^-$/O$_2$), a current density at $E = E^{0\prime}$(OH$^-$/O$_2$) of 0.78 mA cm^{-2}, a fill factor (ff) = 0.51, and a photovoltaic-biased photoelectrochemical ideal regenerative cell efficiency of 0.6%.
© 2016 The Electrochemical Society. [DOI: 10.1149/2.0141605jes] All rights reserved.

Arrays of semiconducting nanowires or microwires provide an interesting morphology for solar fuels generation, due to a minimized ionic transport length between the anode and cathode; the arrangement of individual and complete device units in parallel to provide protection against catastrophic failure in the event that a single device unit fails; reduced materials purity and usage requirements due to orthogonalized directions of light absorption and minority-carrier collection; the ability to decouple optical absorption and catalytic activity of metallic electrocatalysts through strategic placement of the catalyst in the internal volume of the array; and a high internal surface area for facile functional support of earth-abundant electrocatalysts.[1–3] Single-junction Si microwires cannot provide sufficient voltage to perform unassisted solar-driven water splitting (1.23 V at STP), hence tandem core-shell structures or dual microwire array structures are being explored. Theoretical calculations indicate that tandem-junction devices can produce high efficiencies for integrated solar-driven water splitting, hence both planar and non-planar tandem-junction systems have been designed and fabricated.[4–9]

Typical demonstration tandem-junction devices have been fabricated using either a homojunction or heterojunction on a Si microwire core. The core is surrounded by a wide bandgap absorber that forms the second junction, which is generally a semiconductor-liquid junction. Si micro- and nano-wire tandem-junction devices have however exhibited low operating current densities for water splitting, due to the need for large open-circuit voltages (V_{oc}) to overcome the thermodynamic and kinetic requirements for sustained H$_2$(g) and O$_2$(g) production under standard-state conditions.[8,9] WO$_3$ is attractive for a demonstration system because it is acid-stable, as is Si and Nafion, enabling the construction of a fully functional membrane-embedded device for operation in locally acidic conditions.

In such structures, the open-circuit potential (E_{oc}) of the WO$_3$/liquid contact ultimately limits the water-splitting performance of microwire Si/WO$_3$ core-shell tandem devices.[1] Si/WO$_3$ devices fabricated previously also included a tin-doped indium oxide (ITO) layer to provide efficient charge transfer between the Si and WO$_3$, but the ITO layer was unstable under operating conditions and thus limited the ultimate device stability.[1]

Larger E_{oc} values have been obtained from nanowire Si/TiO$_2$ core-shell structures than from microwire Si/WO$_3$ structures because the wide bandgap TiO$_2$ produces a relatively large photovoltage for the device as a whole. In such structures, relatively low E_{oc} values were however observed from the radial Si junction,[8] limiting the observed solar-to-hydrogen (STH) efficiency, η_{STH}, of devices reported to date.

We describe herein the fabrication and properties of a device in which the WO$_3$ has been replaced by TiO$_2$, to generate a larger E_{oc}, and in which the ITO has been replaced by fluorine-doped tin oxide (FTO), to improve the long-term stability of the demonstration device. In conjunction with the high bandgap of TiO$_2$, the presence of a high-quality np$^+$-Si homojunction is expected to result in a larger complete device E_{oc} that should enable higher operating current densities and thus produce improved STH efficiencies in a demonstration-type of device.

np$^+$-Si/FTO/TiO$_2$ devices were fabricated through formation of a radial np$^+$-Si microwire homojunction, followed by sequential deposition of conformal FTO and TiO$_2$ layers (see the Supplementary Information for complete details). Si microwires were first grown on a photolithographically patterned wafer in which 3 μm diameter circular Cu catalysts were deposited in a 7 μm × 7 μm square pattern, with a SiO$_2$ mask layer on the remainder of the Si surface (Figure 1a). The Si microwires were grown using a vapor-liquid-solid (VLS) chemical-vapor deposition (CVD) process in which SiCl$_4$ at 1000 °C in H$_2$(g) was the Si source, and PH$_3$(g) was the n-type dopant source (Figure 1b). The Si microwire arrays were then cleaned using RCA I and II processes to remove organics and metals, respectively, including the remaining Cu catalyst. A SiO$_2$ diffusion barrier was formed at the microwire bases by producing a SiO$_2$ layer using a dry oxidation, masking the bottom of the microwire array with polydimethylsilicon (PDMS), etching the exposed SiO$_2$ in HF(aq), and then removing the PDMS layer (Figure 1c). Radial p$^+$-Si emitters were formed through gas-phase diffusional doping using BCl$_3$ at 950°C in H$_2$(g) (Figure 1d). A conformal FTO layer was then deposited on a Si microwire array via spray pyrolysis of 0.015 M ammonium fluoride and 0.49 M butyltin trichloride in an ethanol/water solution (Figure 1e), while the sample was placed on a hotplate and maintained at 500 °C. Finally, a conformal nano-structured TiO$_2$ layer was deposited at 150 °C for 6 h on the FTO in a hydrothermal process that used an aqueous solution of 0.05 M titanium n-butoxide and 6 M HCl.[10] Subsequent annealing of the array at 450 °C for 30 min resulted in the formation of a nano-structured, conformal rutile TiO$_2$ (Figure 1f) coating. Figure 2 shows scanning-electron micrograph (SEM) images of the structures obtained after the process steps depicted schematically in Figures 1d–1f.

In contact with a non-aqueous ferrocenium/ferrocene redox couple, the np$^+$-Si microwire arrays demonstrated similar performance to arrays reported previously, exhibiting $E_{oc} = -0.483$ V vs the Nernstian potential of the solution, a short-circuit current density (J_{sc}) of 13 mA cm^{-2}, and a fill factor (ff) of 0.48, resulting in an ideal regenerative cell efficiency, η_{IRC}, of 3.0% (Figure S2).[1,11] Contact resistance measurements between p$^+$-Si and FTO performed on planar substrates using the circular transmission line measurement technique (see

*Electrochemical Society Active Member.
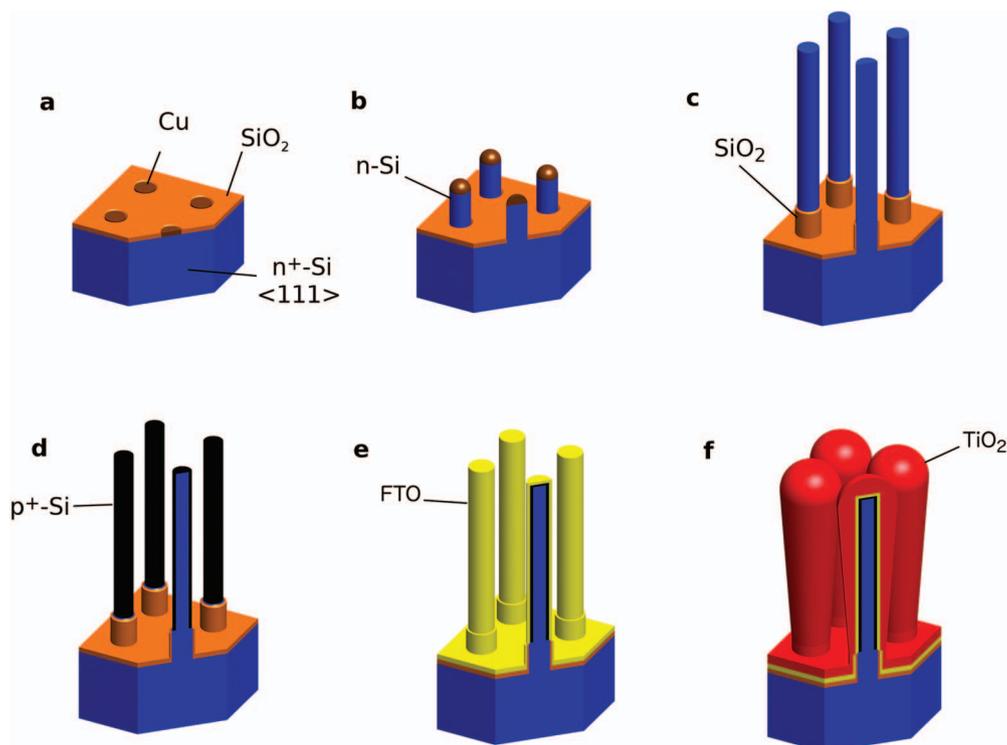^{z}E-mail: haa@caltech.edu; nslewis@caltech.edu

Figure 1. Schematic of the fabrication process. a) 3 μm diameter circular Cu growth catalysts photolithographically patterned in a 7 μm × 7 μm matrix in a 500 nm thick SiO$_2$ layer on an n$^+$-Si (111)-oriented wafer. b) n-Si microwire array growth at 1000°C in a flowing gas consisting of SiCl$_4$ and PH$_3$ in H$_2$. c) Metal and organic cleaned Si microwire array that has a SiO$_2$ diffusion barrier around each wire's base, formed by a dry oxidation of the entire wire array followed by a polymetyldisiloxane mask infill and subsequent etch in HF(aq) to remove the exposed SiO$_2$. d) p$^+$-Si emitter formation by gas phase doping with BCl$_3$. e) Conformal deposition of FTO by spray pyrolysis at 500°C in air. f) TiO$_2$ deposition by an aqueous hydrothermal process followed by a 30 min anneal at 450°C in air.

Supplementary Information for complete details)[12] yielded a specific contact resistance value of 16.6 ± 9.3 Ω cm^2. This resistance corresponds to a ~3 mV voltage loss due to the p$^+$-Si/FTO contact, assuming light-limited current densities of ~2 mA cm^{-2} for rutile TiO$_2$ under Air Mass (AM) 1.5 G illumination conditions and the

~10x surface area increase of Si microwires relative to the area of an analogous planar device. At geometric current densities of ~10 mA cm^{-2}, the voltage losses due to this contact resistance will be ~16 mV and ~160 mV for the Si microwire and planar architectures, respectively. Hence the contact resistance of the p$^+$-Si/FTO interface is sufficiently low to allow use of Si microwire arrays under 1 Sun illumination conditions. However, further contact development is required for planar architectures because a 160 mV contact resistance would significantly affect the overall device performance.

Figure 3 shows the current density versus potential (*J-E*) behavior of p$^+$-Si/FTO/TiO$_2$ microwire arrays in 1.0 M H$_2$SO$_4$(aq) and
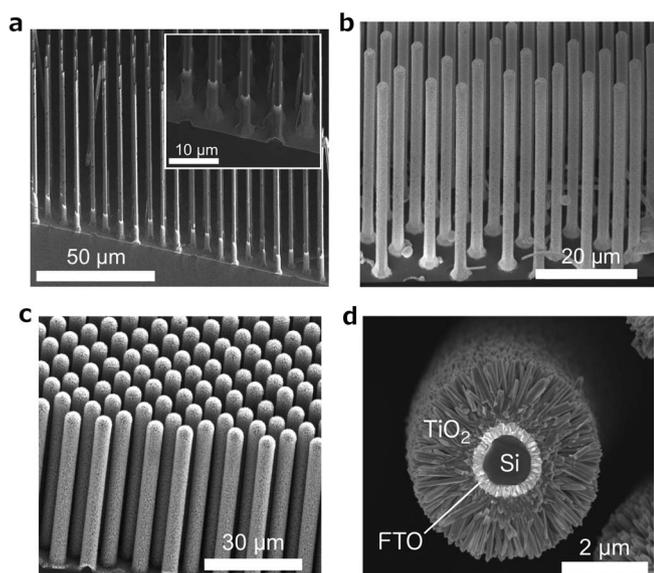

Figure 2. Scanning-electron microscopy (SEM) images showing samples at various stages in the fabrication process. a) A radial junction np$^+$-Si microwire array (Figure 1d). Inset shows a zoomed-in image of the SiO$_2$ diffusion barrier at the bases of the microwires. b) FTO-coated np$^+$-Si microwire array (Figure 1e). c) TiO$_2$-coated np$^+$-Si/FTO microwire array (Figure 1f). d) Cross section of a single np$^+$-Si/FTO/TiO$_2$ microwire with each layer labeled.
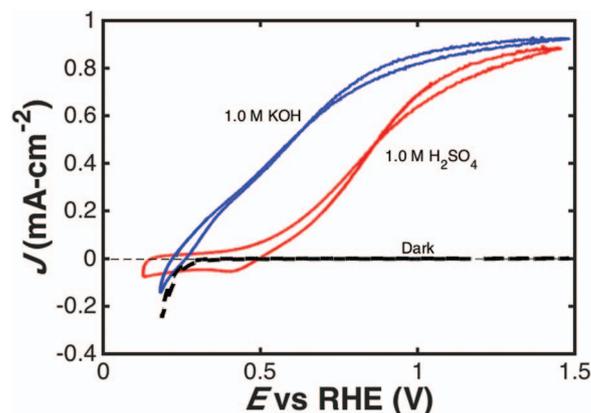

Figure 3. Current density versus potential behavior of p$^+$-Si/FTO/TiO$_2$ microwire array photoelectrodes under dark (1.0 M KOH) and simulated 1 Sun conditions in 1.0 M KOH(aq) and in 1.0 M H$_2$SO$_4$(aq). This behavior demonstrates the superior photoanode performance in 1.0 M KOH, consistent with higher catalytic activity for oxygen evolution on the TiO$_2$ surface in alkaline media relative to under acidic conditions.
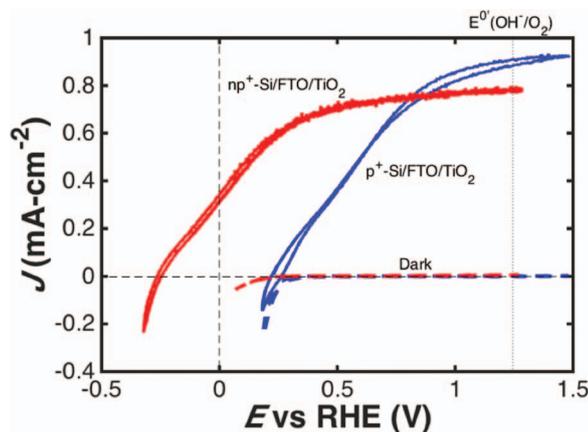
Figure 4. Current density versus potential behavior of p$^+$-Si/FTO/TiO$_2$ and np$^+$-Si/FTO/TiO$_2$ microwire array photoelectrodes in the dark and under simulated 1 Sun conditions. This demonstrates the additive voltage of the tandem junction device and its high E_{OC}, −1.5 V vs $E^{0'}$(OH$^-$/O$_2$), allowing for a relatively high current density of 0.32 mA cm^{-2} at E = −1.23 V vs $E^{0'}$(OH$^-$/O$_2$) (0 V vs RHE).

Figure 5. Current density versus time behavior of np$^+$-Si/FTO/TiO$_2$ microwire array photoelectrodes under simulated 1 Sun conditions and held potentiostatically at 0 V vs RHE. The first run lasted 24 h and was followed by 1 h without illumination at open circuit, in addition to a subsequent 4 hour run under simulated 1 Sun conditions while being held potentiostatically at E = −1.23 V vs $E^{0'}$(OH$^-$/O$_2$) (0 V vs RHE).

1.0 M KOH(aq), respectively, in a three-electrode electrochemical cell configuration. In 1.0 M KOH, p$^+$-Si/FTO/TiO$_2$ microwire arrays, in which the p$^+$-Si microwires acted as a physical scaffold that facilitated evaluation of the performance of the TiO$_2$ in the microwire geometry, exhibited E_{oc} = −1.0 V vs $E^{0'}$(OH$^-$/O$_2$), a current density at $E^{0'}$(OH$^-$/O$_2$) = 0.89 mA cm^{-2}, and ff = 0.39, for a solar-to-oxygen ideal regenerative cell efficiency of η_{IRC} = 0.35% (Figure 4). In contrast, complete np$^+$-Si/FTO/TiO$_2$ core-shell microwire array devices exhibited voltage addition across the series-connected np$^+$-Si and TiO$_2$-liquid junctions, with E_{oc} = −1.41 ± 0.11 V vs $E^{0'}$(OH$^-$/O$_2$), as expected for this tandem junction. The devices exhibited J = 0.62 ± 0.20 mA cm^{-2} at E = $E^{0'}$(OH$^-$/O$_2$) ff = 0.52 ± 0.04, and η_{IRC} = 0.47 ± 0.18% over the 9 photoelectrodes tested. Figure 4 presents the behavior for one of the best-performing devices tested, which exhibited E_{oc} = −1.50 V vs $E^{0'}$(OH$^-$/O$_2$), J = 0.78 mA cm^{-2} at E = $E^{0'}$(OH$^-$/O$_2$), ff = 0.51, and η_{IRC} = 0.60%. Due to the low current densities, this device is expected to operate near 0 V vs the reversible hydrogen electrode (RHE) for unassisted water splitting, and thus ought to exhibit J = 0.32 mA cm^{-2} and η_{STH} = 0.39% in a two-electrode full cell configuration.

The efficiency of complete core-shell np$^+$-Si/FTO/TiO$_2$ microwire-based devices was higher in 1.0 M KOH(aq) than in 1.0 M H$_2$SO$_4$(aq), consistent with the reduced catalytic activity of TiO$_2$ for the oxygen-evolution reaction in acidic media relative to the catalytic activity under alkaline conditions. In contact with 1.0 M H$_2$SO$_4$(aq), addition of an IrO$_2$ electrocatalyst to the TiO$_2$ surface only slightly enhanced the fill factor, in accord with prior work.[8]

Under 1 Sun of simulated sunlight, the current density decreased by ∼15% from its initial value during 24 h of continuous operation under potential control at −1.23 V vs $E^{0'}$(OH$^-$/O$_2$) (0 V vs RHE) (Figure 5). However, when the illumination was discontinued for 1 h and then reestablished, the electrode returned to near its initial performance and subsequently exhibited a similar, albeit slightly lower, current density vs time behavior as that observed in the initial stability measurement. Cyclic voltammograms taken throughout the stability measurement demonstrate a decreased current density near E_{oc} as the measurement progressed (Figure S4). However, at more positive potentials the current density was essentially constant vs time, suggesting that a potential dependent mechanism affects the current density at the most negative potentials. Two possible physical mechanisms consistent with a long time constant and potential dependent behavior include a surface reaction at the TiO$_2$/liquid interface that interferes with catalysis and/or carrier separation and activation of trap states within the TiO$_2$ layer.
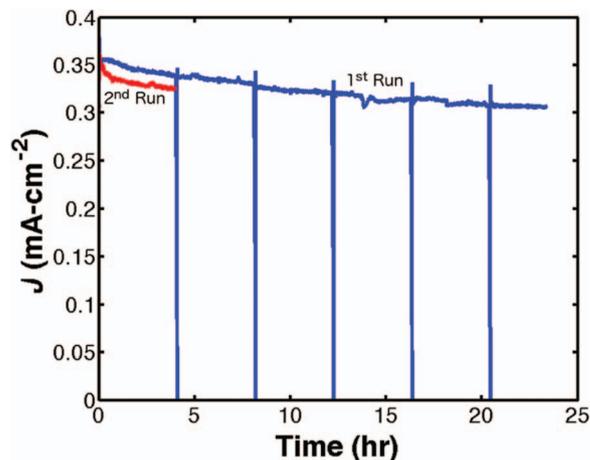
Although the results herein demonstrate an improvement in open-circuit voltage and stability for microwire array devices when used to effect unassisted solar-driven water splitting relative to the behavior of np$^+$-Si microwire/WO$_3$ devices, the bandgap of the TiO$_2$ severely limits the current density achievable under 1 Sun illumination conditions. Accordingly, maintaining the high E_{oc} from the wide-bandgap material while narrowing the bandgap of the top absorber layer is crucial to obtain further significant efficiency improvements, as has been demonstrated in many planar designs.[6,7] To date, incorporation of lower bandgap, high quality materials has been challenging on Si microwire arrays and other similar semiconductor architectures.[13,14]

The combination of material stability and sufficient voltage production has limited and continues to limit microwire and similar three dimensionally structured water splitting device efficiencies. Furthermore, the operational conditions under which the highest performance is achieved further limit options for freestanding device fabrication, such as membrane compatibility. For example, the TiO$_2$ used herein limits operation to aqueous alkaline conditions, which requires an anion exchange membrane to provide ionic conductivity and gas separation capabilities. However, anion exchange membranes remain at the fundamental research level and are not generally designed to be recast in Si microwire arrays while also providing suitable mechanical support when removed from the growth substrate. To-date, attempts to incorporate anion exchange membranes into these devices and thereby obtain a freestanding device failed due to the inability of the membrane casting process to infiltrate the Si microwire array and/or membrane brittleness thwarting attempts to remove the arrays intact from the substrate.

The tandem-junction np$^+$-Si/FTO/TiO$_2$ microwire device reported herein demonstrates an efficiency and stability improvement over previously reported devices. This improvement was achieved by combining two high output-voltage junctions with complementary absorption regimes that simultaneously provide intrinsic stability under the designated operational conditions. Incorporation of an intermediate FTO layer provided a sufficiently low resistance contact between the p$^+$-Si and TiO$_2$. Further efforts to develop compatible anion exchange membranes or to improve the performance in acidic media should provide additional improvements that are necessary for application of freestanding devices in scalable solar-driven water-splitting systems.

Acknowledgments

References

1. M. R. Shaner, K. T. Fountaine, S. Ardo, R. H. Coridan, H. A. Atwater, and N. S. Lewis, *Energy & Environmental Science*, **7**, 779 (2014).
2. B. M. Kayes, H. A. Atwater, and N. S. Lewis, *Journal of Applied Physics*, **97**, 114302 (2005).
3. S. Haussener, C. Xiang, J. M. Spurgeon, S. Ardo, N. S. Lewis, and A. Z. Weber, *Energy & Environmental Science*, **5**, 9922 (2012).
4. S. Hu, C. Xiang, S. Haussener, A. D. Berger, and N. S. Lewis, *Energy & Environmental Science*, **6**, 2984 (2013).
5. J. R. Bolton, S. J. Strickler, and J. S. Connolly, *Nature*, **316**, 495 (1985).
6. O. Khaselev and J. A. Turner, *Science*, **280**, 425 (1998).
7. S. Licht, B. Wang, S. Mukerji, T. Soga, M. Umeno, and H. Tributsch, *Journal of Physical Chemistry B*, **104**, 8920 (2000).
8. C. Liu, J. Tang, H. M. Chen, B. Liu, and P. Yang, *Nano Lett.*, **13**, 2989 (2013).
9. M. T. Mayer, C. Du, and D. Wang, *J. Am. Chem. Soc.*, **134**, 12406 (2012).
10. B. Liu and E. S. Aydil, *J. Am. Chem. Soc.*, **131**, 3985 (2009).
11. M. R. Shaner, S. Hu, K. Sun, and N. S. Lewis, *Energy & Environmental Science*, **8**, 203 (2014).
12. J. H. Klootwijk and C. E. Timmering, *Proc IEEE (ICMTS)*, **17**, 247 (2004).
13. N. C. Strandwitz, D. B. Turner-Evans, A. C. Tamboli, C. T. Chen, H. A. Atwater, and N. S. Lewis, *Adv. Energy Mater.*, **2**, 1109 (2012).
14. C. C. Chen, D. B. Turner-Evans, H. Emmer, S. Aloni, and H. A. Atwater, *39th IEEE Photovoltaic Specialists Conference*, 1 (2013).